Superconducting properties of $RbOs_2O_6$ analyzed within Eliashberg theory

S. Manalo, H. Michor, and G. Hilscher
Institute of Solid State Physics, Technische Universität Wien, Wiedner Hauptstraße 8-10, A-1040 Wien, Austria

M. Brühwiler and B. Batlogg
Laboratory for Solid State Physics, ETH Zürich, 8093 Zürich, Switzerland

(Received 27 January 2006; revised manuscript received 18 April 2006; published 23 June 2006)

Thermodynamic properties such as the specific-heat difference between superconducting and normal states $C_s - C_n$, the thermodynamic critical field $H_c(T)$, and the upper critical field $H_{c2}(T)$ of the β-pyrochlore superconductor $RbOs_2O_6$ are analyzed within the framework of *s*-wave Eliashberg theory including anisotropy and scattering effects, yielding a small electron-phonon coupling anisotropy parameter of about $\langle a_{\mathbf{k}}^2 \rangle \simeq 0.005$, and a Fermi velocity anisotropy parameter $\langle b_{\mathbf{k}}^2 \rangle \simeq 0.3$–$0.35$. Agreement between theory and experiment is achieved for these parameters, the Sommerfeld coefficient γ, and a model spectral function $\alpha^2F(\omega)$ consisting of two Einstein peaks and a Debye contribution. A renormalization of the Fermi velocity by an enhancement factor due to electron-electron correlations $\lambda_{ee} \simeq 1$ is considered in the analysis of the experimental $H_{c2}(T)$ data.

DOI: 10.1103/PhysRevB.73.224520 PACS number(s): 74.25.Bt, 74.70.Dd, 74.62.−c, 74.20.−z

I. INTRODUCTION

In the past years, several experimental results on pyrochlore oxides were published and are of key interest because of their diverse electronic properties, ranging from colossal magnetoresistance to metal-insulator transitions and superconductivity. The first superconductor in the family of pyrochlore oxides was discovered in $Cd_2Re_2O_7$, an α-pyrochlore, with $T_c = 1.0$ K.[1–3] Subsequently, superconductivity was reported in another type of pyrochlore oxide with the general formula AB_2O_6, where *A* is a larger cation and *B* is a smaller transition metal cation, called the β-pyrochlore oxide.[4] KOs_2O_6 (Refs. 5 and 6) has the highest superconducting transition temperature T_c of about 9.6 K, and more reports of superconductivity in the same family of compounds have followed at a rapid pace, with superconductivity being observed in $RbOs_2O_6$ with $T_c = 6.4$ K (Refs. 4 and 7and in $CsOs_2O_6$ with $T_c = 3.3$ K.[8]

While the underlying mechanism of superconductivity in $Cd_2Re_2O_7$ can be understood within the weak coupling Bardeen, Cooper, and Schrieffer (BCS) theory, there is still an ongoing discussion concerning the pairing mechanism in $RbOs_2O_6$ and KOs_2O_6. Given the fact that both systems are expected to have very similar electronic properties, their different behavior poses an interesting question on whether the pairing mechanism is different in the two compounds[9,10]. The rather large difference of critical temperatures cannot be fully explained by the difference in superconducting parameters and electronic properties in the conventional *s*-wave pairing framework.[9,11] An analysis of the dynamical stability of these compounds shows significant anharmonicity of the alkali ion displacement most pronounced in KOs_2O_6 and less in $RbOs_2O_6$ and $CsOs_2O_6$, which could add to the difference in T_c's.[12] Based on the results of specific-heat measurements, Brühwiler *et al.* suggested that $RbOs_2O_6$ is a conventional BCS-type superconductor in the intermediate coupling regime.[7,13] Pressure effects on the transition temperature and the magnetic field penetration depth[14,15] and NMRmeasurements[16] give further support to their conclusions. On the other hand and based on an analysis of the upper critical field obtained from resistivity measurements, Hiroi and co-workers suggested unconventional superconductivity for KOs_2O_6.[6,17] Koda and co-workers further substantiated this suggestion with a probe by muon spin rotation and suggested the pairing to be mediated by spin fluctuations.[18]

While the role of spin fluctuations and details of the order parameter symmetry need to be fully elucidated in KOs_2O_6, apparently $RbOs_2O_6$ is an *s*-wave superconductor with an anisotropic, nodeless gap.[10] A crossover from BCS to charged critical behavior was found near T_c by Schneider *et al.*[19] Based on the results of NMR measurements on $RbOs_2O_6$, Magishi *et al.*[16] estimated the anisotropy of the conventional *s*-wave gap to be $\langle a^2 \rangle = 0.25$ by fits of their results to the weak coupling BCS expectations for an anisotropic and isotropic gap. These results and the pronounced anharmonicity of the alkali ion displacement of $RbOs_2O_6$ motivated us to estimate the anisotropy of the pairing mechanism by analyzing the experimental data within the framework of Eliashberg theory,[20] which treats superconductivity as a boson-exchange phenomenon and has often been applied to describe conventional anisotropic superconductors.[21–23] The central quantity in this theory is the electron-phonon interaction spectral function $\alpha^2F(\omega)$ which can be determined from tunneling experiments[24] or theoretically from band structure calculations. Using such an $\alpha^2F(\omega)$ within Eliashberg theory allows to reproduce the superconducting properties of a conventional superconductor within experimental accuracy.

In this paper we present investigations of the thermodynamic properties and of the upper critical field $H_{c2}(T)$ of $RbOs_2O_6$. Results on the critical temperature, the specific heat using condensation energy analysis (CEA),[13] and the temperature dependence of the upper critical magnetic field were analyzed using an anisotropic model of the *s*-wave Eliashberg formalism. As there are no data available which would allow us to determine the electron-phonon interaction spectral density $\alpha^2F(\omega)$ directly by inversion, we have developed a model spectral function consisting of two Einstein

modes and a Debye contribution to optimally describe the measured thermodynamic properties and upper critical field.

In Sec. II, we show the theoretical background used for the analysis. An analysis of the experimental data in terms of the anisotropic Eliashberg theory is discussed in Sec. III. Conclusions are drawn in Sec. IV.

II. THEORY

The theoretical approach towards a theory of anisotropic polycrystalline superconductors within the framework of Eliashberg theory is based on the separable model for the anisotropic electron-phonon interaction introduced by Markovitz and Kadanoff[25] which was extended by Daams and Carbotte[26] to describe an anisotropic electron-phonon interaction spectral function,

$$\alpha^2F(\omega)_{\mathbf{k},\mathbf{k}'} = (1 + a_{\mathbf{k}})\alpha^2F(\omega)(1 + a_{\mathbf{k}'}), \tag{1}$$

where $\mathbf{k}$ and $\mathbf{k}'$ are the incoming and outgoing quasiparticle momentum vectors in the electron-phonon scattering process and $a_{\mathbf{k}}$ is an anisotropy function with the important feature $\langle a_{\mathbf{k}}\rangle = 0$, where $\langle\cdots\rangle$ denotes the Fermi surface average over k ($\langle\cdots\rangle'$ is the average over k'). As anisotropy effects are generally assumed to be rather small, it is sufficient to keep the mean square anisotropy $\langle a^2\rangle$ as the important anisotropy parameter. Finally, $\alpha^2F(\omega)$ is the electron-phonon interaction spectral density of the equivalent isotropic system, where $a_{\mathbf{k}} = 0$.

A. Thermodynamic properties

Thermodynamic properties of a superconductor are calculated from the free energy difference ΔF between the superconducting and normal state,[27]

$$\Delta F = -\pi TN(E_F)\frac{1}{2}\sum_n^{\omega_c}\left\langle\left(\sqrt{\tilde{\omega}_{\mathbf{k}}^2(\omega_n) + \tilde{\Delta}_{\mathbf{k}}^2(\omega_n)} - |\tilde{\omega}_{\mathbf{k}}(\omega_n)|\right)\times\left(1 - \frac{|\tilde{\omega}_{\mathbf{k}}^0(\omega_n)|}{\sqrt{\tilde{\omega}_{\mathbf{k}}^2(\omega_n) + \tilde{\Delta}_{\mathbf{k}}^2(\omega_n)}}\right)\right\rangle, \tag{2}$$

with the quasiparticle density of states $N(E_F)$ at the Fermi level, which we obtain from the Sommerfeld coefficient γ in this work. $N(E_F)$ is therefore an effective density of states corresponding to the band structure result $N(E_F)_{\mathrm{bs}}$ enhanced by a coupling constant λ_{ee} due to electronic interaction $N(E_F) = N(E_F)_{\mathrm{bs}}(1 + \lambda_{ee})$. The renormalized quasiparticle frequencies $\tilde{\omega}_{\mathbf{k}}(\omega_n)$ and the Matsubara gaps $\tilde{\Delta}_{\mathbf{k}}(\omega_n)$ are the solutions of the nonlinear s-wave Eliashberg equations,

$$\tilde{\omega}_{\mathbf{k}}(\omega_n) = \omega_n + \pi T\sum_m^{\omega_c}\left\langle\left(\lambda_{\mathbf{k},\mathbf{k}'}(m-n) + \delta_{m,n}\frac{t^+_{\mathbf{k},\mathbf{k}'}}{T}\right)\times\frac{\tilde{\omega}_{\mathbf{k}'}(\omega_m)}{\sqrt{\tilde{\omega}_{\mathbf{k}'}^2(\omega_m) + \tilde{\Delta}_{\mathbf{k}'}^2(\omega_m)}}\right\rangle', \tag{3}$$

$$\tilde{\Delta}_{\mathbf{k}}(\omega_n) = \pi T\sum_m^{\omega_c}\left\langle\left(\lambda_{\mathbf{k},\mathbf{k}'}(m-n) - \mu^\star_{\mathbf{k},\mathbf{k}'} + \delta_{m,n}\frac{t^+_{\mathbf{k},\mathbf{k}'}}{T}\right)\frac{\tilde{\Delta}_{\mathbf{k}'}(\omega_m)}{\sqrt{\tilde{\omega}_{\mathbf{k}'}^2(\omega_m) + \tilde{\Delta}_{\mathbf{k}'}^2(\omega_m)}}\right\rangle'. \tag{4}$$

The $\omega^0_{\mathbf{k}}(\omega_n)$ are the normal state quasiparticle frequencies determined by

$$\tilde{\omega}^0_{\mathbf{k}}(\omega_n) = \omega_n + \pi T\sum_m^{\omega_c}\left\langle\lambda_{\mathbf{k},\mathbf{k}'}(m-n) + \delta_{m,n}\frac{t^+_{\mathbf{k},\mathbf{k}'}}{T}\right\rangle' \times \mathrm{sgn}\ \omega_m. \tag{5}$$

In these equations ω_c, the cutoff frequency, is usually an integer multiple of the Debye frequency of the system, $\omega_n = \pi T(2n+1), n = 0, \pm1, \pm2, \ldots$, $t^+_{\mathbf{k},\mathbf{k}'} = 1/[2\pi(\tau_{\mathrm{tr}})_{\mathbf{k},\mathbf{k}'}]$ is the anisotropic scattering rate due to inelastic impurity scattering with $(\tau_{\mathrm{tr}})_{\mathbf{k},\mathbf{k}'}$ as the anisotropic transport relaxation time, $\mu^\star_{\mathbf{k},\mathbf{k}'}$ is the anisotropic Coulomb pseudopotential, and

$$\lambda_{\mathbf{k},\mathbf{k}'}(m-n) = 2\int_0^\infty d\Omega\frac{\Omega\alpha^2F(\Omega)_{\mathbf{k},\mathbf{k}'}}{\Omega^2 + (\omega_m - \omega_n)^2}. \tag{6}$$

In the case of weak anisotropy effects the $\mathbf{k},\mathbf{k}'$ dependence of the Coulomb pseudopotential and of the impurity scattering is neglected and the anisotropy of the Matsubara gaps is described by the ansatz

$$\tilde{\Delta}_{\mathbf{k}}(\omega_n) = \tilde{\Delta}_0(\omega_n) + a_{\mathbf{k}}\tilde{\Delta}_1(\omega_n), \tag{7}$$

with $\tilde{\Delta}_i(\omega_n)$, $i = 0, 1$, being isotropic functions. In applying Eq. (7) to Eq. (4) only terms of the order of $\langle a^2\rangle$ are kept.

B. Upper critical field

The upper critical field $H_{c2}(T)$ of an anisotropic polycrystalline superconductor employs, in addition, a separable ansatz to describe the anisotropy of the Fermi velocity $v_{F,\mathbf{k}}$,[28]

$$v_{F,\mathbf{k}} = (1 + b_{\mathbf{k}})\langle v_F\rangle, \tag{8}$$

with $\langle v_F\rangle$ the isotropic Fermi velocity. $b_{\mathbf{k}}$ is an anisotropy function defined in the same way as $a_{\mathbf{k}}$. Again, only terms of the order $\langle b^2\rangle$ are kept in case of small anisotropy effects. The upper critical field in its temperature dependence is then described by the following set of equations:[28]

$$\tilde{\Delta}_{\mathbf{k}}(\omega_n) = \pi T\sum_m(1 + a_{\mathbf{k}})\lambda(m-n)\langle(1 + a_{\mathbf{k}'})\tilde{\Delta}_{\mathbf{k}'}(\omega_m)\chi_{\mathbf{k}'}(m)\rangle' - \pi T\sum_m\left(\mu^\star - \delta_{n,m}\frac{t^+}{T}\right)\langle\tilde{\Delta}_{\mathbf{k}'}(\omega_m)\chi_{\mathbf{k}'}(m)\rangle', \tag{9}$$

$$\chi_{\mathbf{k}}(n) = \frac{2}{\sqrt{\alpha_{\mathbf{k}}}}\int_0^\infty dx e^{-x^2}\tan^{-1}\left(\frac{\sqrt{\alpha_{\mathbf{k}}}x}{|\tilde{\omega}_{\mathbf{k}}(\omega_n)|}\right), \tag{10}$$

and

$$\alpha_{\mathbf{k}} = \frac{e}{2} H_{c2}(T)(1 + b_{\mathbf{k}})^2 \langle v_F \rangle^2. \quad (11)$$

N-band models have been extensively studied as a tool to describe anisotropic features of superconductors. The separable model employed in this work can be described in its simplest form by a Fermi surface split into two half-spheres of equal weight

$$P(a) = \delta(-a)/2 + \delta(a)/2, \quad (12)$$

with radii $r \pm a$, if r is the radius of the equivalent isotropic Fermi sphere.[29] Using the Fermi surface harmonics (FSH) notation introduced by Allen,[30] Daams[31] observed that this separable model is equivalently described by a restriction to zeroth-order FSH in each of the two subregions of the Fermi surface. According to their work, the separable model applied in further calculations of this work corresponds to a two-band model in which the two Fermi surface regions have equal weight.

In the case of the upper critical field any deviation from the equal weight configuration causes $H_{c2}(T)$ to approach the isotropic case. Furthermore, the relative signs of $a_{\mathbf{k}}$ and $b_{\mathbf{k}}$ in the same Fermi-surface sheet are also of importance to the analysis of H_{c2}. B and structure calculations can give a good estimate for the weight and the relative signs of $a_{\mathbf{k}}$ and $b_{\mathbf{k}}$ in the corresponding regions of the Fermi surface. With the knowledge of the Fermi surface consisting of two dominant sheets and the shape of the experimental upper critical field favouring opposite signs of $a_{\mathbf{k}}$ and $b_{\mathbf{k}}$ within the same sheets, we used equal weights for the two Fermi surface regions and opposite signs of $a_{\mathbf{k}}$ and $b_{\mathbf{k}}$ in the following analysis.

C. Impurity scattering

A clean limit analysis can only be a first step which allows us to put some margins on the various anisotropy parameters. Within Eliashberg theory, impurities are treated in Born's limit[32] which assumes the impurities to be randomly distributed and to be of dilute concentration. In such a limit impurities are characterized by a scattering rate t_+ which is proportional to the impurities' concentration. Their main effect is the smearing out of the electron-phonon interaction anisotropy resulting in a reduction of T_c depending on the value of $\langle a_{\mathbf{k}}^2 \rangle$,[25] an enhancement of H_{c2} at low temperatures, and a reduction of the high temperature upward curvature of H_{c2} as was demonstrated by Weber *et al.*[21] for Nb. They applied the standard procedure to determine the anisotropy parameters by doping the sample under investigation in a controlled way with some impurities and to measure the change in T_c and in the residual resistivity ρ_n as a function of impurity concentration. This gives another, rather reliable estimate for the anisotropy parameter $\langle a^2 \rangle$ (Ref. 25) and allows us to calculate the impurity parameter t^+ which enters Eqs. (4) and (9) from the Drude relation $t^+ = \rho_n \hbar \omega_p / 8\pi^2$, with the plasma frequency of a free electron gas $\omega_p = 4\pi n e^2/m$, where n is the density, m and e are the mass and charge of an electron. An analysis of the T_c versus t_+ dependence with respect to $\langle a_{\mathbf{k}}^2 \rangle$ is shown below.

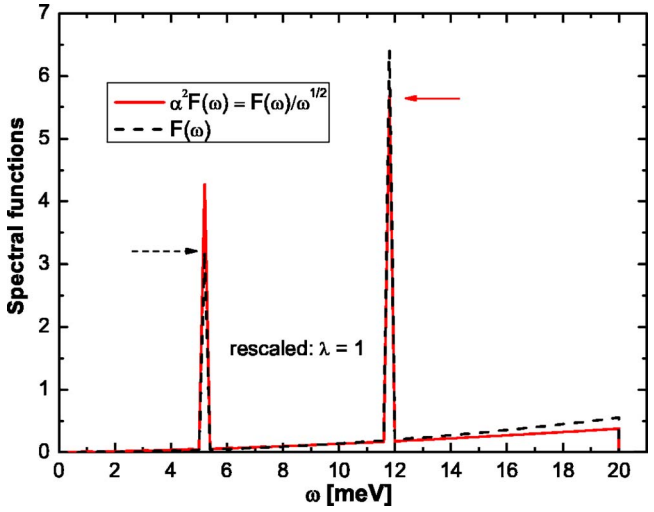

FIG. 1. (Color online) Model phonon spectrum $F(\omega)$ and electron-phonon spectral function $\alpha^2 F(\omega)$, with $\alpha^2(\omega) = 1/\sqrt{\omega}$. The functions were rescaled to obtain a coupling parameter of $\lambda = 1.0$.

III. RESULTS AND DISCUSSION

A. Spectral function

It would be standard procedure to start with an electron-phonon interaction spectral density $\alpha^2 F(\omega)$ directly by inversion of tunneling data by means of the McMillan-Rowell tunneling inversion method. As there are no data available which would allow us to determine $\alpha^2 F(\omega)$ directly, we started with a model spectrum consisting of two Einstein peaks given by Hiroi *et al.*[33] at 5.3 meV and 11.9 meV with an amplitude ratio of 1:2 for the Rb and Os atoms, which they obtained by fitting the lattice specific heat to the experimental data of $RbOs_2O_6$.

Carbotte's concept of an optimal electron-phonon interaction spectral density as an Einstein spectrum, which allows us to describe all physical properties of a superconductor in an optimal way[34] can be applied to anisotropic superconductors, as was shown by Manalo and Schachinger,[35] using the borocarbides $LuNi_2B_2C$ and YNi_2B_2C as examples. An Einstein spectrum is sufficient for clean-limit systems; a 2δ-peak spectrum is better suited for anisotropic systems with impurities.

In the course of the present analysis the data could not be modelled appropriately with only two δ functions. It was necessary to account for the O oscillations by either varying the ratios between the given peaks, placing a third δ function at higher frequencies or adding a Debye spectrum. As an arbitrary choice, the contributions to the phonon spectrum area were weighted with the number of atoms per formula unit 1:9, 2:9 for the 5.3, 11.9 peaks and 6:9 for the Debye spectrum (Fig. 1). The spectrum was cut off at a Debye temperature of $\Theta_D = 240$ K.[7]

As a first test, this model phonon spectrum $F(\omega)$ was taken as a substitute for $\alpha^2 F(\omega)$ to calculate the thermodynamic properties. It was rescaled with a constant, such that the electron-phonon coupling strength

TABLE I. Input parameters of the analysis with Eliashberg theory. The Sommerfeld coefficient γ, the lattice parameter a of the cubic structure, and the Debye temperature Θ_D were used to calculate the thermodynamic properties. The mean Fermi velocity $\langle v_F \rangle$ is needed for $H_{c2}(T)$.

γ [mJ/(mol K^2)]	44
a (Å)	10.114
T_c (K)	6.37
Θ_D (K)	240
$\langle v_F \rangle$ (cm/s)	2.587×10^7

$$\lambda_{ep} = 2\int_0^\infty d\omega \frac{\alpha^2 F(\omega)}{\omega} \tag{13}$$

gives $\lambda_{ep}=1$, the value estimated from the specific heat jump at T_c.[13] In the isotropic case with $\langle a^2 \rangle = 0$ and $T_c=6.37$ K, the Coulomb pseudopotential μ^* is slightly greater than 0.2, and the results showed good agreement with the experimental data.

However, the phonon contribution to the specific heat yields information on $F(\omega)$ rather than on $\alpha^2 F(\omega)$. We made the same assumption for $RbOs_2O_6$ as Junod *et al.*[36] on the form of the electron-phonon coupling function $\alpha^2(\omega) \sim \omega^{-1/2}$ for the A15 compounds. A consistent description of the upper critical field and thermodynamic properties of borocarbide superconductors within Eliashberg theory was also achieved with the same function.[22,35]

We apply this method to the model phonon spectrum of $RbOs_2O_6$ and find the resulting spectral function $\alpha^2 F(\omega)$, rescaled such that $\lambda_{ep}=1$, to be suitable to describe the thermodynamic properties of $RbOs_2O_6$ in the superconducting regime. With this spectral function (Fig. 1), $T_c=6.37$ and in the isotropic case, the Coulomb pseudopotential is $\mu^*=0.165$, a value which lies well within the usual range of 0.1–0.2.

Thermodynamic properties

The thermodynamic properties of $RbOs_2O_6$ were calculated with the parameters given in Table I. The lattice parameter a of the cubic structure was taken from Ref. 37, and the Sommerfeld coefficient $\gamma=44$ mJ/(mol K^2) was obtained from the specific heat data by means of CEA.[13]

The thermodynamic critical field $H_c(T)$ is calculated from the experimental data by integrating the difference between the zero-field and 12 T measurement, i.e., the lattice contribution to the zero-field heat capacity cancels out in $\Delta C = C_s - C_n \hat{=} C(0\ \mathrm{T}) - C(12\ \mathrm{T})$ which is used in the analysis below. In the numerical calculations, the thermodynamic critical field $H_c(T)$ is calculated from the free energy difference $\Delta F = F_s - F_n$,

$$H_c(T) = \sqrt{-2\Delta F/\mu_0}, \tag{14}$$

and the specific heat difference ΔC is related to ΔF through

$$\Delta C(T) = -T\frac{\partial^2 \Delta F(T)}{\partial T^2}. \tag{15}$$

The specific heat experimental data (sample F in Ref. 13) was rescaled with a factor ~ 1.3 to account for a 100% superconducting phase. The thermodynamic critical field $H_c(T)/H_c(0)$ obtained from the specific heat difference was multiplied with $H_c(0)=124.9$ mT.[13] Comparison of the numerical results for $C_s - C_n$, $H_c(T)$, and the deviation function $D(T/T_c)$ of the thermodynamic critical field

$$D(T/T_c) = \frac{H_c(T)}{H_c(0)} - \left[1 - \left(\frac{T}{T_c}\right)^2\right], \tag{16}$$

with experimental data show fairly good agreement even for the isotropic case, which improves with increasing anisotropy values $\langle a^2 \rangle$. Anisotropy affects primarily the deviation function as can be seen in Fig. 2. An increase of $\langle a^2 \rangle$ results in a shift of the maximum deviation from the purely parabolic dependence of $H_c(T)$ to larger negative values. Numerical results with an anisotropy parameter $\langle a^2 \rangle = 0.001$ lie above, and those with $\langle a^2 \rangle = 0.005$ in the clean-limit case lie below the experimental data, but are still within the error bars. The latter result from experimental error bars of the specific heat data and primarily from the extrapolation of $H_c(T)$ to $T \to 0$.

B. Upper critical field $H_{c2}(T)$

The average Fermi velocity and its anisotropy parameter enter the Eliashberg equations via Eq. (8). While the curvature of H_{c2} at T_c is mainly influenced by the anisotropy parameters $\langle a^2 \rangle$ and $\langle b^2 \rangle$, the average Fermi velocity is of key importance for the magnitude of $H_{c2}(0)$. A smaller $\langle v_F \rangle$ results in a higher $H_{c2}(0)$ and vice versa. Saniz[39] estimated the average Fermi velocity $\langle v_F \rangle$ from electronic structure calculations to be 2.587×10^7 cm/s for $RbOs_2O_6$. In the clean limit and isotropic case, the zero temperature upper critical field $H_{c2}(0)$ calculated with the bare and average Fermi velocity is very low at ~ 0.6 T. We have to keep in mind that adding impurities increases $H_{c2}(T)$ even in isotropic systems.[28,38] Moreover, adding impurities "smears out" the anisotropy[25] which results in an additional increase of $H_{c2}(T)$, and, furthermore, in a less pronounced upward curvature of $H_{c2}(T)$ close to T_c (Ref. 21) if $\langle a^2 \rangle$ and $\langle b^2 \rangle$ are kept constant in the calculations. In order to increase $H_{c2}(T)$ in the clean-limit calculations, it is therefore necessary to take impurity scattering into account. With the given average Fermi velocity for $RbOs_2O_6$, it is possible to increase $H_{c2}(T)$ to fit the experimental data at low temperatures by adding a considerable amount of impurity scattering ($t_+=10$ meV). However, the overall temperature behavior of H_{c2} cannot be described with such high impurity scattering, because any reasonable contribution of anisotropy is "smeared out."

The density of states obtained from band structure calculations $N(E_F)_{bs}=4.9$ states/eV f.u. (Refs. 9 and 12) results in a Sommerfeld coefficient $\gamma_{bs}=11.56$ mJ/mol K^2, with the relation $\gamma = \pi^2 k_B^2 N(E_F)/3$. This value is about one fourth of the

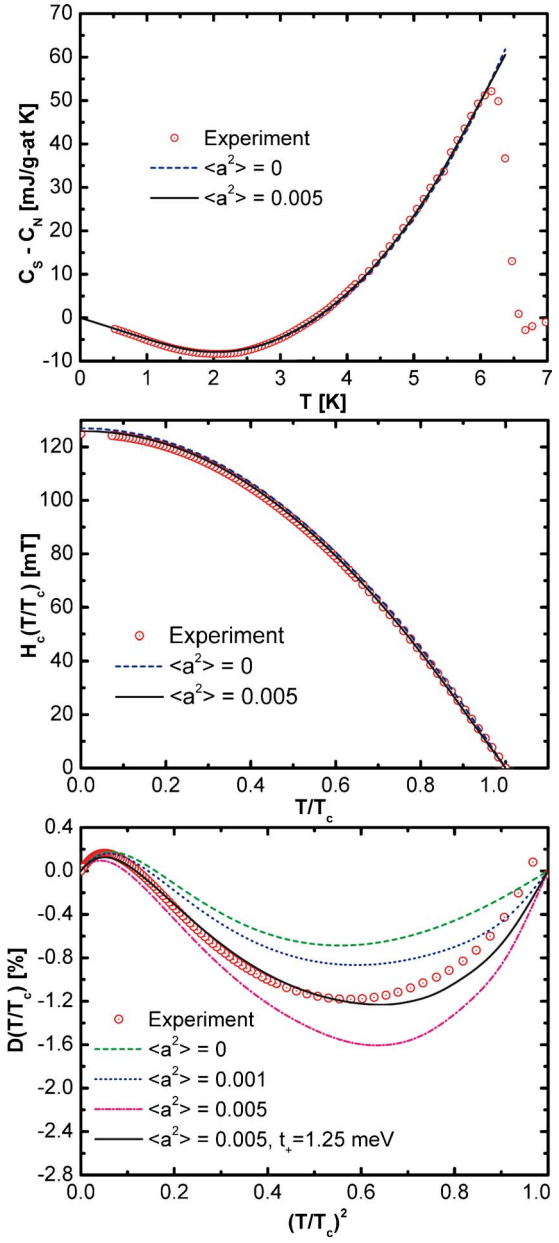

FIG. 2. (Color online) Specific heat difference between superconducting and normal states $C_s - C_n$, thermodynamic critical field $H_c(T/T_c)$, and deviation function $D(T/T_c)$ for the isotropic case and with anisotropy values of $\langle a^2\rangle = 0.001, 0.005$ in the clean limit, and with an impurity parameter $t_+ = 1.25$ meV for $\langle a^2\rangle = 0.005$.

result obtained from specific heat measurements $\gamma = 44$ mJ/(mol K^2), which corresponds to $N(E_F) = 18.7$ states/(eV f.u.). In this system, an effective Sommerfeld coefficient can be given as

$$\gamma^* = \frac{\pi^2}{3} k_B^2 N(E_F)(1+\lambda_{ep})(1+\lambda_{ee}), \tag{17}$$

with the enhancement factor ascribed to electron-electron correlations λ_{ee}, of which the maximum value $\lambda_{ee} \simeq 1$ is given in Ref. 13 (corresponding to λ_c). The origin of the significant electron-electron mass enhancement is discussed

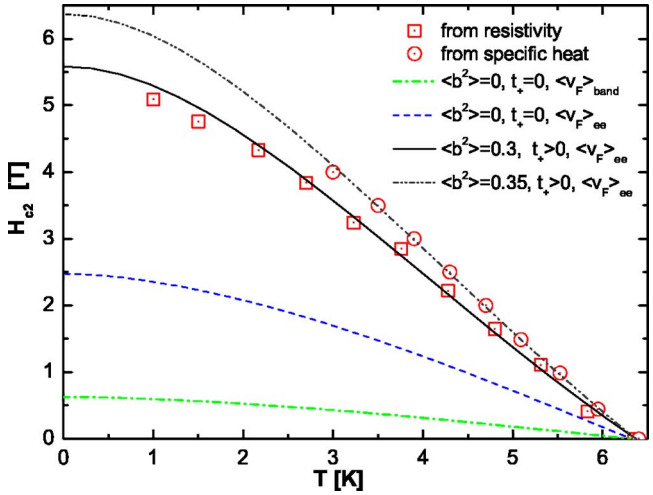

FIG. 3. (Color online) Upper critical field $H_{c2}(T)$ in the isotropic and clean limit case ($t_+ = 0$) with the bare Fermi velocity $\langle v_F\rangle = 2.587 \times 10^7$ cm/s and the effective Fermi velocity $\langle v_F\rangle_{ee} = 1.294 \times 10^7$ cm/s. The fit to the experimental resistivity data was achieved with the effective Fermi velocity, an anisotropy parameter of $\langle a^2\rangle = 0.005$, Fermi velocity anisotropy parameter $\langle b^2\rangle = 0.3$, and an impurity scattering parameter $t_+ = 1.25$ meV. The corresponding results for the specific heat data are $\langle a^2\rangle = 0.005$, $\langle b^2\rangle = 0.35$, and $t_+ = 1.85$ meV.

in Ref. 40, where λ_{ee} values estimated from specific heat data of $RbOs_2O_6$ with $\lambda_{ee} \simeq 1$ and KOs_2O_6 with $\lambda_{ee} \simeq 1.7$, are analyzed in the context with the growing anharmonicity and frustrated geometry in these compounds. It is an interesting question if this additional enhancement is seen in the upper critical field $H_{c2}(T)$. In such a case, the enhancement enters the calculations through a rescaling factor of the average Fermi velocity

$$\langle v_F\rangle_{ee} = \frac{\langle v_F\rangle}{1+\lambda_{ee}}. \tag{18}$$

The numerical results for the critical field in the clean limit and isotropic case with the renormalized average Fermi velocity $\langle v_F\rangle_{ee} = 1.294 \times 10^7$ cm/s are shown in Fig. 3. With this value for the average Fermi velocity, $H_{c2}(0)$ is increased to 2.5 T and a fit to $H_{c2}(T)$ from resistivity data can be achieved with $\langle a^2\rangle = 0.005$, $\langle b^2\rangle = 0.3$, and $t_+ = 1.25$ meV. The experimental $H_{c2}(T)$ data obtained from specific heat measurements,[13] which are less sensitive to grain boundary effects and thus yield an accurate bulk measure for $T_c(H)$, are shown for comparison and can be described with $\langle a^2\rangle = 0.005$, $\langle b^2\rangle = 0.35$, and $t_+ = 1.85$ meV. As a consequence, we presume these results to be limits for the Fermi velocity $\langle v_F\rangle_{ee} \geq 1.29 \times 10^7$ cm/s, its anisotropy parameter $\langle b^2\rangle = 0.3-0.35$, and the impurity scattering parameter $t_+ = 1.25-1.85$. With this value for t_+ and an anisotropy parameter $\langle a^2\rangle = 0.005$, the deviation function is even closer to the experimental data (Fig. 2). The results of the analysis are given in Table II.

The stable value of the critical temperature T_c compared to the large difference in upper critical field $H_{c2}(0)$ values

TABLE II. A consistent description within Eliashberg theory was achieved with the above anisotropy parameters $\langle a^2\rangle$, $\langle b^2\rangle$ and impurity content t_+. The model phonon spectrum was rescaled, such that $\lambda_{ep}=1$. The mean Fermi velocity was renormalized by λ_{ee}.

λ_{ep}	1.0
μ^*	0.165
$\langle a^2\rangle$	0.005
$\langle b^2\rangle$	0.3–0.35
t_+ (meV)	1.25–1.85 (l=43–64 nm)
λ_{ee}	1.0

obtained by different groups[4,13,17] indicates, that $\langle a^2\rangle$ is rather small. We calculated $T_c(t_+)$ for various anisotropy parameters $\langle a^2\rangle$ with the conditions given above. For $\langle a^2\rangle=0.005$, the critical temperature of a clean sample is $T_{c0}\simeq 6.39$ K and approaches 6.34 K in the dirty limit. In case of higher anisotropy values, T_c is more sensitive to an increase of t_+ (see Fig. 4). Based on fits of BCS expectations to NMR measurements, Magishi *et al.*[16] estimated an anisotropy parameter of $\langle a^2\rangle\simeq 0.25$, which would result in T_c changes in the range of about 2.7 K if inserted in the above calculations. Considering the rather stable value of the critical temperature T_c found in different samples, it seems unlikely that the anisotropy value exceeds $\langle a^2\rangle=0.01$. Furthermore, a consistent description of thermodynamic properties and $H_{c2}(T)$ of $RbOs_2O_6$ within Eliashberg theory is hardly possible with larger values.

The scattering rate is related to the transport relaxation time via $t_+=1/\tau_{tr}$. With $\langle v_F\rangle_{ee}=l/\tau_{tr}$ and $t_+=1.25-1.85$ meV (Table II), we can estimate the mean free path with $l=\langle v_F\rangle_{ee}/t_+$, to be $l\simeq 43-64$ nm. This rather small value may be attributed to the presence of defects at the oxygen sites. Yonezawa *et al.*[4,17] estimated the upper critical field for $RbOs_2O_6$ based on resistivity measurements on their sample to be $H_{c2}(0)\sim 10$ T. This higher value may be caused by different experimental methods and/or stronger impurity scattering. While surface effects could play a role in resistivity measurements, they do not affect the specific heat. Assuming that the higher critical field value[4,17] of 10 T is only caused by impurity scattering, a scattering rate of $t_+=4.1$ meV (l=20 nm) is required. A rough estimate of the mean free path can also be made with the BCS-Pippard coherence length $\xi_0=\hbar\langle v_F\rangle/\pi\Delta$ and the Ginzburg Landau coherence length $\xi^{-1}=\xi_0^{-1}+l^{-1}$, where $2\Delta/k_BT_c=3.87$ and $\xi=7.4$ nm,[13] which results in $l\simeq 10$ nm. Based on these results, we suggest a reasonable interval for the mean free path in this system to be 10–100 nm

IV. CONCLUSION

Thermodynamic properties such as the specific-heat difference between superconducting and normal states C_s-C_n, the thermodynamic critical field $H_c(T)$, and the upper critical field $H_{c2}(T)$ of the β-pyrochlore superconductor $RbOs_2O_6$ were analyzed within the framework of *s*-wave Eliashberg theory. The consistent description of these properties is only possible if anisotropy and scattering effects are included. We were able to describe the experimental data with a model spectral function $\alpha^2F(\omega)$ consisting of two Einstein and a Debye contribution, an electron-phonon coupling factor $\lambda_{ep}=1$, and a Coulomb pseudopotential $\mu^*=0.166$. Measures for the anisotropy parameter of the electron-phonon interaction $\langle a^2\rangle=0.005$, and the mean anisotropy parameter of the Fermi velocity $\langle b^2\rangle=0.3-0.35$ can be given as a result of the fits of thermodynamic properties and the upper critical field $H_{c2}(T)$.

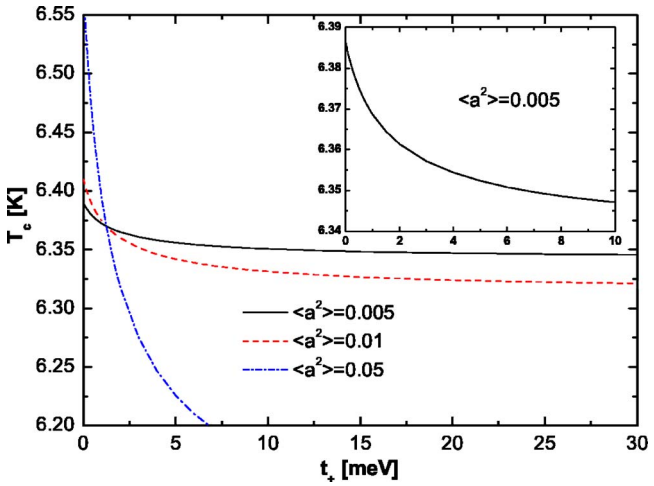

FIG. 4. (Color online) Dependence of T_c on the impurity scattering rate t_+ for various anisotropy parameters $\langle a^2\rangle$. The plots were calculated with the condition $T_c=6.37$ at $t_+=1.25$ meV.

Impurity scattering plays a major role with respect to $H_{c2}(T)$. It may also contribute to different zero temperature upper critical field values obtained by different groups.[4,13,17] With the above anisotropy parameters and a renormalized mean Fermi velocity $\langle v_F\rangle_{ee}=1.294\times 10^7$ cm/s, the $H_{c2}(T)$ data can be described with a scattering rate of $t_+=1.25-1.85$ meV, which corresponds to a mean free path $l\simeq 64-43$ nm. The description of the upper critical field within Eliashberg theory was only possible under consideration of a renormalized Fermi velocity, with $\lambda_{ee}\simeq 1$, and indicates that the additional enhancement of the Sommerfeld coefficient γ as compared to band structure calculations is also observed in the upper critical field.

ACKNOWLEDGMENTS

We thank E. Schachinger for helpful inputs concerning the analysis with Eliashberg theory, and R. Saniz for providing the mean Fermi velocity of $RbOs_2O_6$ prior to publication. This work was supported by the Austrian Science Foundation FWF under Grant No. P 16250.

[1] M. Hanawa, Y. Muraoka, T. Tayama, T. Sakakibara, J. Yamaura, and Z. Hiroi, Phys. Rev. Lett. **87**, 187001 (2001).
[2] H. Sakai, K. Yoshimura, H. Ohno, H. Kato, S. Kambe, R. E. Walstedt, T. D. Matsuda, Y. Haga, and Y. Onuki, J. Phys.: Condens. Matter **13**, L785 (2001).
[3] R. Jin, J. He, S. McCall, C. S. Alexander, F. Drymiotis, and D. Mandrus, Phys. Rev. B **64**, 180503(R) (2001).
[4] S. Yonezawa, Y. Muraoka, Y. Matsushita, and Z. Hiroi, J. Phys. Soc. Jpn. **73**, 819 (2004).
[5] S. Yonezawa, Y. Muraoka, Y. Matsushita, and Z. Hiroi, J. Phys.: Condens. Matter **16**, L9 (2004).
[6] Z. Hiroi, S. Yonezawa, and Y. Muraoka, J. Phys. Soc. Jpn. **73**, 1651 (2004).
[7] M. Brühwiler, S. M. Kazakov, N. D. Zhigadlo, J. Karpinski, and B. Batlogg, Phys. Rev. B **70**, 020503(R) (2004).
[8] S. Yonezawa, Y. Muraoka, and Z. Hiroi, J. Phys. Soc. Jpn. **73**, 1655 (2004).
[9] R. Saniz, J. E. Medvedeva, Lin-Hui Ye, T. Shishidou, and A. J. Freeman, Phys. Rev. B **70**, 100505(R) (2004).
[10] K. Arai, J. Kikuchi, K. Kodama, M. Takigawa, S. Yonezawa, Y. Muraoka, and Z. Hiroi, Physica B **359–361**, 488 (2005).
[11] R. Saniz and A. J. Freeman, Phys. Rev. B **72**, 024522 (2005).
[12] J. Kunes, T. Jeong, and W. E. Pickett, Phys. Rev. B **70**, 174510 (2004).
[13] M. Brühwiler, S. M. Kazakov, J. Karpinski, and B. Batlogg, Phys. Rev. B **71**, 214517 (2005).
[14] R. Khasanov, D. G. Eshchenko, J. Karpinski, S. M. Kazakov, N. D. Zhigadlo, R. Brütsch, D. Gavillet, D. Di Castro, A. Shengelaya, F. La Mattina, A. Maisuradze, C. Baines, and H. Keller, Phys. Rev. Lett. **93**, 157004 (2004).
[15] T. Muramatsu, N. Takeshita, C. Terakura, H. Takagi, Y. Tokura, S. Yonezawa, Y. Muraoka, and Z. Hiroi, Phys. Rev. Lett. **95**, 167004 (2005).
[16] K. Magishi, J. L. Gavilano, B. Pedrini, J. Hinderer, M. Weller, H. R. Ott, S. M. Kazakov, and J. Karpinski, Phys. Rev. B **71**, 024524 (2005).
[17] Z. Hiroi, S. Yonezawa, J. Yamaura, T. Muramatsu, Y. Matsushita, and Y. I. Muraoka, J. Phys. Soc. Jpn. **74**, 3400 (2005).
[18] A. Koda, W. Higemoto, K. Ohishi, S. R. Saha, R. Kadono, S. Yonezawa, Y. Muraoka, and Z. Hiroi, J. Phys. Soc. Jpn. **74**, 1678 (2005).
[19] T. Schneider, R. Khasanov, and H. Keller, Phys. Rev. Lett. **94**, 077002 (2005).
[20] G. M. Eliashberg, Sov. Phys. JETP **11**, 696 (1960).
[21] H. W. Weber, E. Seidl, C. Laa, E. Schachinger, M. Prohammer, A. Junod, and D. Eckert, Phys. Rev. B **44**, 7585 (1991).
[22] S. Manalo, H. Michor, M. El-Hagary, G. Hilscher, and E. Schachinger, Phys. Rev. B **63**, 104508 (2001).
[23] M. Zehetmayer, H. W. Weber, and E. Schachinger, J. Low Temp. Phys. **133**, 407 (2003).
[24] W. L. McMillan and J. M. Rowell, Phys. Rev. Lett. **14**, 108 (1965).
[25] D. Markovitz and L. P. Kadanoff, Phys. Rev. **131**, 563 (1963).
[26] J. M. Daams and J. P. Carbotte, J. Low Temp. Phys. **43**, 263 (1981).
[27] J. Bardeen and M. Stephen, Phys. Rev. **136**, A1485 (1964).
[28] M. Prohammer and E. Schachinger, Phys. Rev. B **36**, 8353 (1987).
[29] L. Niel, N. Giesinger, H. W. Weber, and E. Schachinger, Phys. Rev. B **32**, 2976 (1985).
[30] P. B. Allen, Phys. Rev. B **13**, 1416 (1976).
[31] J. M. Daams, Ph.D. thesis, McMaster University, Ontario, 1977.
[32] V. Ambegaokar, in *Superconductivity*, edited by R. D. Parks (Marcel Dekker, New York, 1969), p. 259.
[33] Z. Hiroi, S. Yonezawa, T. Muramatsu, J. Yamaura, and Y. Muraoka, J. Phys. Soc. Jpn. **74**, 1255 (2005).
[34] J. P. Carbotte, Rev. Mod. Phys. **62**, 1027 (1990).
[35] S. Manalo and E. Schachinger, J. Low Temp. Phys. **123**, 149 (2001).
[36] A. Junod, T. Jarlborg, and J. Muller, Phys. Rev. B **27**, 1568 (1983).
[37] S. M. Kazakov, N. D. Zhigadlo, M. Brühwiler, B. Batlogg, and J. Karpinski, Supercond. Sci. Technol. **17**, 1169 (2004).
[38] N. R. Werthammer, E. Helfand, and P. C. Hohenberg, Phys. Rev. **147**, 295 (1966).
[39] R. Saniz (private communication). This value corresponds to the purely "intraband" plasma frequency. In an EELS experiment, the effective plasma frequency results from intraband and additional contributions by interband transitions and can be different from the one related to the average Fermi velocity. See also G. Maksimov, I. I. Mazin, S. N. Rashkeev, and Y. A. Uspenski, J. Phys. F: Met. Phys. **18**, 833 (1988).
[40] M. Brühwiler, S. M. Kazakov, J. Karpinski, and B. Batlogg, Phys. Rev. B **73**, 094518 (2006).